

# Solid-state NMR and IR for the analysis of pharmaceutical solids: polymorphs of fosinopril sodium\*

HARRY G. BRITTAIN,† KENNETH R. MORRIS, DAVID E. BUGAY, AJIT B. THAKUR and ABU T.M. SERAJUDDIN

*Bristol-Myers Squibb Pharmaceutical Research Institute, P.O. Box 191, New Brunswick, NJ 08903, USA.*

**Abstract:** The two polymorphic modifications of fosinopril sodium have been characterized as to their differences in melting behaviour, powder X-ray diffraction patterns, Fourier transform infrared spectra (FTIR), and solid-state  $^{31}\text{P}$ - and  $^{13}\text{C}$ -NMR spectra. The polymorphs were found to be enantiotropically related based upon melting point, heat of fusion, and solution mediated transformation data. Analysis of the solid-state FTIR and  $^{13}\text{C}$ -NMR data indicated that the environment of the acetal side chain of fosinopril sodium differed in two polymorphs, and that there might be *cis-trans* isomerization about the  $\text{C}_6\text{-N}$  peptide bond. These conformational differences are postulated as the origin of the observed polymorphism.

**Keywords:** *Fosinopril sodium; polymorphism; infrared spectroscopy; solid-state  $^{13}\text{C}$ - and  $^{31}\text{P}$ -NMR; thermal analysis; powder X-ray diffraction.*

## Introduction

Identification and characterization of the possible polymorphic behaviour in a drug substance is an essential aspect of drug development. It is well known that the improper selection of a polymorph, or any polymorphic change in the dosage form, can adversely influence the bio-availability, processability, and stability of a formulation [1]. Although single crystal X-ray diffraction is the best method for the characterization of polymorphs, it is often difficult to produce crystals of sufficiently high crystallographic quality for all polymorphic phases. As a result, the polymorphism of pharmaceutical compounds is normally characterized on the basis of thermal behaviour, solubility, dissolution rate, and crystallographic properties [1, 2].

Infrared spectroscopy (IR) is finding wide use in the study of polymorphic behaviour, with differences in vibrational modes being used to differentiate between crystal polymorphs [3, 4]. The changes in vibrational frequencies arise when the spatial relation of functional groups is not equivalent in alternate

structures. Solid-state nuclear magnetic resonance (NMR) spectrometry has also been used in the study of polymorphism [4, 5], since the resonance frequency of nuclei will differ when their spatial relations are changed as a result of variations in the molecular packing.

Since solid-state IR and NMR spectroscopies can be used to probe the nature of polymorphism on the molecular level, these methods would be particularly useful in instances where full crystallographic characterization of polymorphs was not found to be possible. This situation has been encountered in the particular instance of fosinopril sodium, an angiotensin converting enzyme (ACE) inhibitor [6]. The structure of this compound is shown in Fig. 1, together with a numbering scheme useful for the identification of each atom. Fosinopril sodium has been found to exist in two anhydrous polymorphic forms, denoted as the A- and B-phases. Although the structure of the A-phase has been determined from an analysis of its single crystal, it has not been possible to generate crystals of sufficient quality to permit the solving of the B-phase structure.

\* Presented at the 'Fourth International Symposium on Pharmaceutical and Biomedical Analysis', April 1993, Baltimore, MD, USA.

† Author to whom correspondence should be addressed.

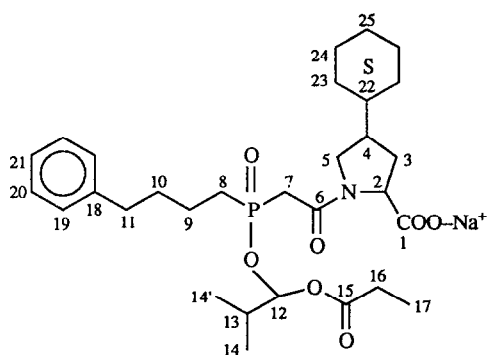


**Figure 1**  
Fosinopril sodium structure and numbering scheme used throughout the text.

In the present work, we present details of the conventional evaluation of these polymorphs, and describe how solid-state IR and NMR spectroscopies were used to deduce the molecular changes associated with the polymorphism.

## Materials and Methods

### Preparation of polymorphs

Fosinopril sodium was produced by the Chemical Process Development Division of Bristol-Myers Squibb Company. The A-phase was obtained by crystallization from various organic solvents such as acetone, acetonitrile, and some alcohols or their mixtures with water. The formation of this phase was independent of the solvent used as long as the crystallization step was sufficiently slow. The B-phase was obtained by the rapid vacuum concentration on drying of a solution of the A-phase from an organic solvent. The B-phase obtained in this manner may, however, contain a small amount of the A-phase. A pure sample of the B-phase was produced by flash evaporation on a watch glass. In this method, a solution of 0.5 g of A-phase material in 10 ml of methanol was poured on a large watch glass, the solvent was evaporated with a jet of filtered air, and the solid obtained was dried in an oven at 60°C for 1 h to remove any residual solvent. Thermogravimetric analysis of isolated materials showed less than 0.1% total volatile content remaining in either form. Neither form was found to be hygroscopic, and no hydrate species have ever been detected during the analysis of numerous samples.

### Powder X-ray diffraction (XRD)

Powder X-ray diffraction patterns were obtained using a Philips model APD 3720 powder diffraction system, equipped with a vertical goniometer in the  $\theta/2-\theta$  geometry. The X-ray generator (Philips model XRG 31000) was operated at 45 kV and 40 mA, using the K-alpha line of copper at 1.544056 Å as the radiation source. Each sample was scanned between 2 and 32° 2- $\theta$ , at a scan rate of 0.04° 2- $\theta$  s<sup>-1</sup>, and in step sizes of 0.04° 2- $\theta$ .

### Thermal properties

Measurements of differential scanning calorimetry (DSC) and thermogravimetry (TG) were obtained on a TA Instruments model 9900 thermal analysis system. Approximately 1.5 mg samples were accurately weighed into a DSC pan, the pans hermetically sealed, and a pinhole punched into the pan lid. The use of the pinhole allows for pressure release, but still ensures that the thermal reactions proceed under controlled conditions. For TG determinations, approximately 10 mg of sample was placed on the pan, and inserted in the TG furnace. For either measurement, the samples were heated at a rate of 10°C min<sup>-1</sup>, up to a final temperature of 200°C.

### Solid-state FTIR

Qualitative diffuse reflectance spectra were acquired on a Nicolet model 740 FTIR spectrophotometer, interfaced with a Spectra-Tech, Inc., Collector™ diffuse reflectance accessory unit. A water cooled global source was used in conjunction with a Ge/KBr beamsplitter and a deuterated triglycine sulphate (DTGS) detector. Each 13 mm sample cup was filled with pure material and levelled by lightly pressing a glass slide downward upon the sample until the sample height matched the cup height. Dried KBr was used for the background data set. Each spectrum represents 64 co-added scans obtained at a spectral resolution of 1 cm<sup>-1</sup>. The frequency domain spectra were obtained by ratioing the background data set against the sample data set. This produced a spectrum in per cent reflectance units, which was converted to log (1/R). This procedure is analogous to per cent transmittance/absorbance unit data representation.

### Solid-state NMR

The solid-state <sup>13</sup>C- and <sup>31</sup>P-NMR spectra

were obtained on a Bruker AM-250 spectrometer utilizing the resonant frequencies of 62.89 and 101.26 MHz, respectively. Approximately 400 mg of sample was used to fill the zirconium rotors, which were sealed with a Kel-F cap. Each sample was spun at the magic angle, at the frequency of  $5.0 \pm 0.02$  kHz. The magic angle setting was calibrated by the KBr method [7].

The cross polarization, magic angle spinning (CP/MAS) pulse sequence was used to acquire qualitative  $^{13}\text{C}$ -NMR spectra [8–10]. Each spectrum represents 128 transients (4 K data set, spectral width of 20,000 Hz, 5 s recycle time, 2 ms contact time,  $6.2 \mu\text{s}$  pulse width) acquired under phase cycling conditions which minimize baseline and intensity artifacts. The Hartmann–Hahn match was optimized by monitoring the  $^{13}\text{C}$  intensity versus  $^{13}\text{C}$  rf field with a spinning adamantane sample. The data set was subjected to an exponential weighting function of 5.0 Hz to improve the signal-to-noise ratio [11, 12]. Fourier transformation and phase correction of the free induction decay then produced a frequency domain spectrum. All spectra were recorded at ambient temperature, and the chemical shifts were externally referenced to tetramethylsilane ( $\delta(\text{CH}_3)_4\text{Si} = \delta(\text{adamantane CH}_2) - 38.3$ ).

A single pulse, high powered decoupling pulse sequence was employed for qualitative  $^{31}\text{P}$ -NMR data acquisition. Analogous to the  $^{13}\text{C}$ -NMR spectra, 128 transients were co-

added (4 k data set, spectral width of 50,000 Hz, 5 s recycle time,  $4.9 \mu\text{s}$  pulse width) under phase cycling conditions. Subsequent digital filtering (line broadening factor of 5 Hz), Fourier transformation, and phase correction produced a frequency domain spectrum. The spectra were recorded at ambient temperature and externally referenced to ammonium phosphate ( $\text{NH}_4\text{H}_2\text{PO}_4$ ). In order to investigate the possibility of dipolar coupling in the  $^{31}\text{P}$ -NMR spectra, a second set of solid-state spectra were obtained on a modified Nicolet 150 spectrometer utilizing the  $^{31}\text{P}$  resonant frequency of 60.72 MHz. These spectra were obtained under the following conditions: 3.6 kHz spin rate, 500 transients, 20000 Hz spectral width, 2 K data set, and externally referenced to 85% phosphoric acid.

## Results and Discussion

The powder X-ray diffraction (XRD) patterns of the two polymorphs of fosinopril sodium are shown in Fig. 2. Full summaries of scattering angles, d-spacings, and relative peak intensities are provided in Tables 1 and 2. The most obvious differences in the XRD patterns of the two polymorphs were noted at low scattering angles which are associated with crystal planes separately by relatively large distances. This portion of the powder patterns was used for identification of the two polymorphic forms.

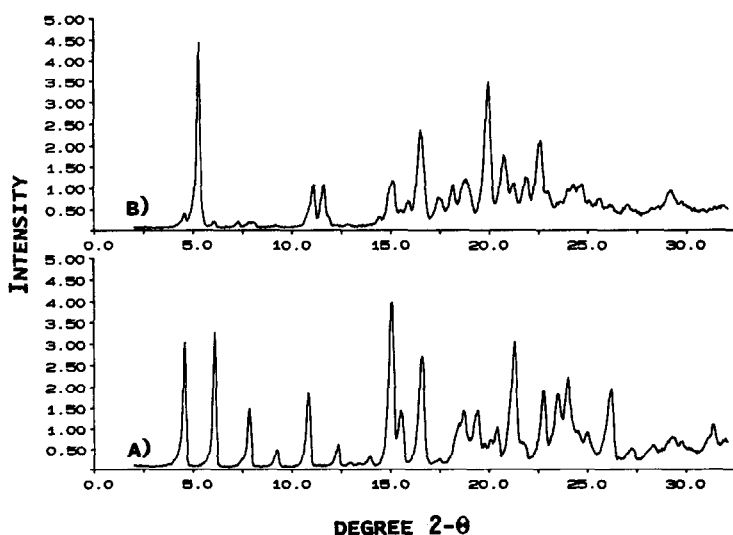


**Figure 2**  
Powder X-ray diffraction patterns for the two polymorphic forms of fosinopril sodium: (A) A-phase, (B) B-phase.

**Table 1**  
Crystallographic data for fosinopril sodium, A-phase

Angle (degrees 2- $\theta$ )	D-spacing (Å)	Rel. intensity ( $I/I_{max}$ )
4.5625	19.3515	66.63
6.0625	14.5664	38.16
7.8050	11.3179	25.52
9.1825	9.6229	13.07
10.7825	8.1983	52.05
12.2400	7.2251	6.57
12.8600	6.8782	1.11
13.8825	6.3738	6.95
14.9500	5.9210	100.00
15.4675	5.7240	39.64
16.5075	5.3657	55.75
18.6025	4.7658	39.27
19.2700	4.6022	27.10
19.9525	4.4463	5.27
20.3000	4.3710	10.05
21.1475	4.1977	53.78
21.7050	4.0911	4.49
22.6375	3.9247	40.77
23.3450	3.8073	46.24
23.8725	3.7243	36.00
24.4200	3.6421	2.37
26.0550	3.4171	27.82
27.1350	3.2835	3.27
28.1900	3.1630	8.87
29.2800	3.0477	11.81
29.6625	3.0092	3.82
30.2150	2.9554	1.44
31.2050	2.8639	9.77
31.8075	2.8110	7.43

**Table 2**  
Crystallographic data for fosinopril sodium, B-phase

Angle (degrees 2- $\theta$ )	D-spacing (Å)	Rel. intensity ( $I/I_{max}$ )
5.3000	16.6602	100.00
7.2625	12.1620	3.11
8.0600	10.9604	2.79
11.0625	7.9914	24.15
11.5650	7.6453	23.54
12.7725	6.9251	0.91
14.3500	6.1672	5.12
14.8500	5.9606	19.63
15.0800	5.8702	25.87
15.8425	5.5894	11.78
16.4875	5.3721	51.28
17.3950	5.0939	13.56
18.0950	4.8983	20.19
18.6675	4.7494	22.49
18.9650	4.6756	15.83
19.8800	4.4624	76.87
20.6750	4.2925	35.89
21.1600	4.1952	20.19
21.8025	4.0730	23.54
22.4975	3.9488	44.79
22.9450	3.8728	14.25
23.8925	3.7213	15.46
24.1575	3.6810	18.27
24.6125	3.6140	18.41
25.0000	3.5589	9.16
25.5300	3.4862	10.43
26.0625	3.4161	6.00
26.9125	3.3101	6.55
29.0950	3.0666	13.79
30.7150	2.9085	1.64

The thermal properties of the two fosinopril sodium polymorphs were studied through the use of differential scanning calorimetry. The melting endotherm of the A-phase was observed at approximately 197°C, while the melting endotherm associated with the B-phase was noted at 200°C. Through integration of the endothermic events, it was determined that the corresponding enthalpies of fusion were 61 and 54 J g<sup>-1</sup>, respectively. High-performance liquid chromatographic analysis performed on materials recovered immediately after melting indicated that no significant degradation took place upon melting, if the sample temperature was not allowed to rise much past the melting point. This finding indicates that the thermodynamic data deduced from the thermal studies is not compromised by sample decomposition. The thermal data also indicates that the two polymorphs of fosinopril sodium are enantiotropic in nature. According to the heat of fusion rule, the higher melting polymorph of an enantiotropic system would exhibit the lower heat of fusion [13].

It was established that the A-phase of fosinopril sodium was the most stable polymorph at room temperature. This was deduced by equilibrating excess amounts of A-phase, B-phase, and mixtures of these in acetone or methanol (with and without water). After 1–3 days of equilibration, the solids were recovered and analysed by XRD to determine the resulting polymorphic content. In all instances, the B-phase had converted to the A-phase. It was found that the A-phase could not be transformed into the B-phase through any physical process, except by the use of flash evaporation of alcoholic solutions. Samples of B-phase stored in the solid state were also found to convert eventually into A-phase material, although this process was found to require months for measurable conversion to take place.

Mid-IR spectra, obtained using diffuse reflectance, for the A- and B-phases of fosinopril sodium are shown in Fig. 3. As would be anticipated from the existence of differing crystal structures, the IR spectra exhibited significant differences in the observed

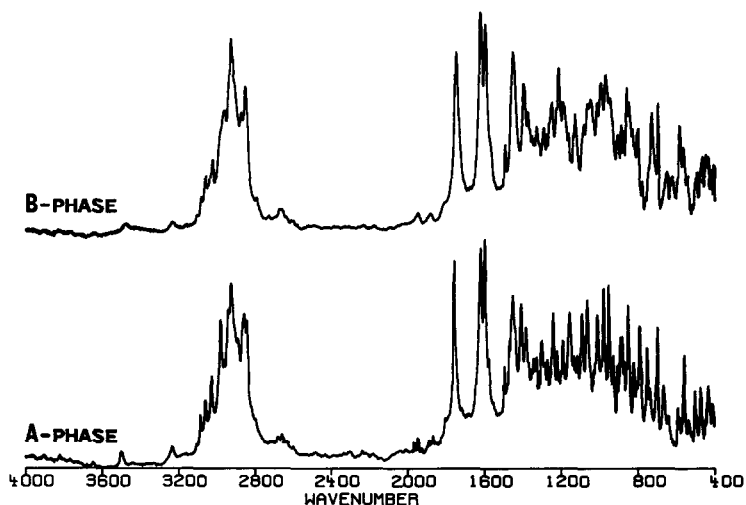


**Figure 3**  
Diffuse reflectance, mid-IR spectra of the A- and B-phases of fosinopril sodium.

vibrational transitions. The most important differences were noted in the carbonyl region, and the observed frequencies are compared in Table 3. It was observed that the carbonyl frequency corresponding to the group at C<sub>15</sub> was significantly different in the two polymorphs, while the frequencies for the C<sub>6</sub> and C<sub>1</sub> carbonyls were equivalent in the two polymorphs.

The solid-state <sup>13</sup>C-NMR spectra obtained for the A- and B-phases of fosinopril sodium are shown in Fig. 4. Since portions of the

molecule are conformationally different in the two phases and consequently exist in slightly different chemical environments, it would be anticipated that identical nuclei in each polymorphic modification could display different resonance positions. Spectral differences were found to be most significant in the C—H aliphatic, C—C aliphatic, and carbonyl regions. The observed chemical shifts are compared in Table 3. Based upon an initial evaluation of the spectral data, it was concluded that the chemical shifts of carbons C<sub>12</sub>, C<sub>14</sub>, C<sub>14'</sub>, C<sub>15</sub> and C<sub>17</sub> were different for the A- and B-phases, while the chemical shifts associated with carbons C<sub>2</sub>, C<sub>5</sub>, C<sub>18</sub>, C<sub>19</sub>, C<sub>19'</sub>, C<sub>20</sub>, C<sub>20'</sub> and C<sub>21</sub> were equivalent in the two polymorphs. This data suggests that the polymorphism of fosinopril sodium originates from conformational differences in the acetal side chain.

It is also plausible that the origin of the crystallographic polymorphism could be due to a *cis-trans* isomerization about the proline peptide bond, C<sub>6</sub>—N [T. Siahaan, personal communication]. Opella has shown that the chemical shifts of the β and γ carbons of the proline moiety are shifted based upon a *cis* or *trans* configuration of the C<sub>6</sub>—N peptide bond [14]. The structural feature of fosinopril sodium is very similar to a X-proline dipeptide (where X = an amino acid). Upon inspection of the NMR spectra for the A- and B-phases of fosinopril sodium, major spectral differences are indeed noted in the region of 20–40 ppm, where the β (C<sub>3</sub>) and γ (C<sub>4</sub>) carbons resonate.

**Table 3**  
Spectroscopic properties of fosinopril sodium in its polymorphic forms

Assignment	A-phase	B-phase
(a) Carbonyl stretching frequencies		
C <sub>1</sub>	1600 cm <sup>-1</sup>	1598
C <sub>6</sub>	1622	1621
C <sub>15</sub>	1759	1753
(b) <sup>13</sup> C Resonances, C—H aliphatic region		
C <sub>14</sub> , C <sub>14'</sub>	19.6, 20.7 ppm*	14.9, 16.2
C <sub>17</sub>	7.9	11.8
(c) <sup>13</sup> C Resonances, C—C aliphatic region		
C <sub>2</sub>	63.6 ppm	63.8
C <sub>5</sub>	52.2	52.4
C <sub>12</sub>	100.4	94.2
C <sub>18</sub>	142.8	142.7
C <sub>19</sub> , C <sub>19'</sub> , C <sub>20</sub> , C <sub>20'</sub> , C <sub>21</sub>	125.2	126.6
(d) <sup>13</sup> C Resonances, carbonyl region		
C <sub>1</sub>	178.0 ppm	176.4
C <sub>6</sub>	164.5	164.3
C <sub>15</sub>	171.5	172.6

\* All <sup>13</sup>C chemical shifts externally referenced to TMS.

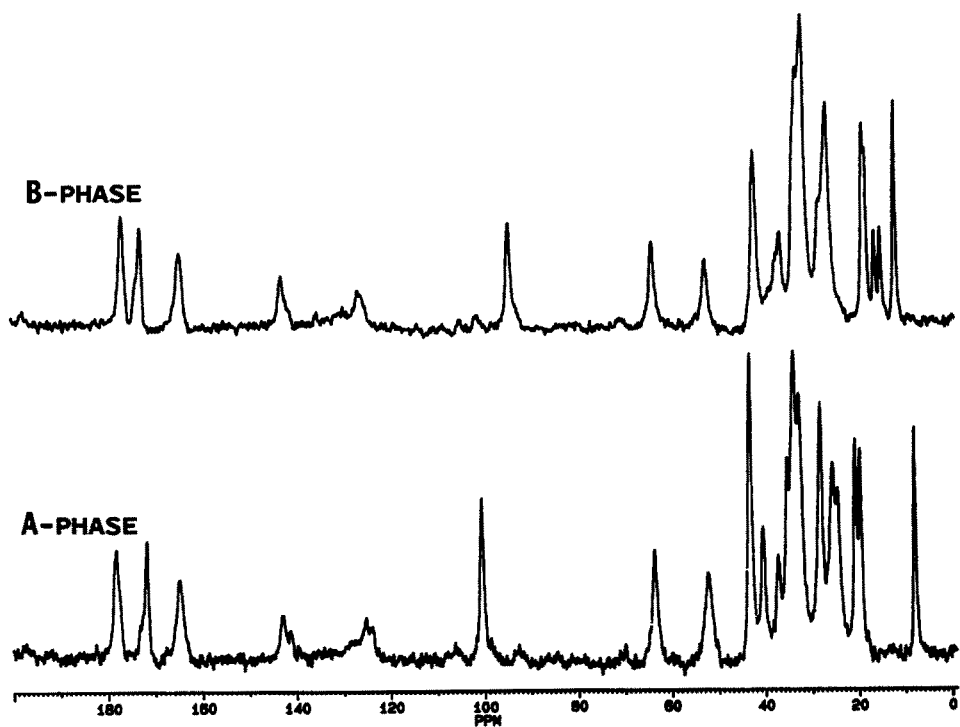


Figure 4  
Solid-state  $^{13}\text{C}$  CP/MAS NMR spectra of the two fosinopril sodium polymorphs.

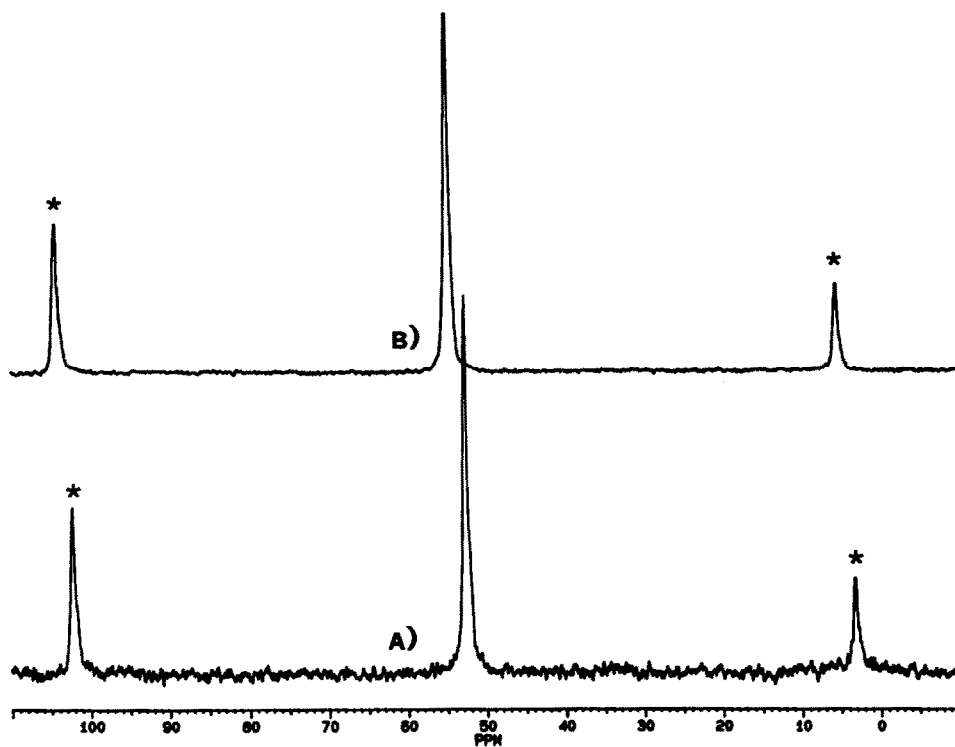


Figure 5  
Solid-state  $^{31}\text{P}$ -NMR spectra for: (A) A-phase and (B) B-phase of fosinopril sodium. Spinning sidebands are designated by asterisks.

Unfortunately, due to severe spectral overlap, unequivocal assignment of the C<sub>3</sub> and C<sub>4</sub> nuclei was not possible, even after spectral editing techniques. Although a full solid-state NMR spectral assignment could not be made, it may be concluded from the NMR data that the polymorphism of fosinopril sodium originates from conformational differences in the acetal side chain, and possibly due to *cis-trans* isomerization about the C<sub>6</sub>—N peptide bond.

The solid-state <sup>31</sup>P-NMR spectra for A- and B-phase fosinopril sodium are displayed in Fig. 5. The significant chemical shift difference between the A- and B-phase resonances (A-phase,  $\delta = 52.8$ ; B-phase,  $\delta = 55.0$  ppm) demonstrates the existence of distinct chemical environments for the phosphorus nuclei in each polymorph. Upon close inspection of the respective resonances, a shoulder resonance was detected. For each pair of resonances, the splitting between the main resonance and the shoulder was approximately 88 Hz. The origin of the shoulder resonance may be attributed to either: (a) crystallographic/magnetic inequivalency of phosphorus atoms in the unit cell, or (b) quadrupolar coupling to the cyclohexylproline nitrogen nucleus. Since quadrupolar effects are inversely proportional to magnetic field strength [15], <sup>31</sup>P-NMR spectra of the two polymorphs were obtained at a lower field (60.72 MHz). The splitting between the main resonance and the shoulder was found to increase to 145 Hz at the lower field, and some peak broadening was also noted. These results are consistent with field-dependent broadening effects resulting from quadrupolar coupling as opposed to magnetic inequivalency.

## Conclusions

Fosinopril sodium exists as one of two crystalline anhydrous polymorphs, which are enantiotropic with respect to each other, and readily identifiable on the basis of their X-ray diffraction powder patterns. The two poly-

morphs exhibit significant differences in both their solid-state NMR and IR spectra. The spectral data indicate that the acetal side chain nuclei (composed of the C<sub>12</sub> through C<sub>17</sub> grouping) are not equivalent in the two polymorphs. The NMR data also suggest that the conformational differences between the two physical forms may be due to *cis-trans* isomerization along the C<sub>6</sub>—N peptide bond.

*Acknowledgements* — The authors wish to thank Susan J. Bogdanowich and Joseph DeVincentis for help in acquiring the XRD data. We would also like to acknowledge the efforts of the Colorado State University Regional NMR Center, funded by National Science Foundation Grant No. CHE-8616437, for the series of solid-state <sup>31</sup>P-NMR spectra obtained at 60.72 MHz.

## References

- [1] J. Haleblan and W. McCrone, *J. Pharm. Sci.* **58**, 911–929 (1969).
- [2] J.K. Haleblan, *J. Pharm. Sci.* **64**, 1269–1288 (1975).
- [3] M. Kuhnert-Brandstätter and H.W. Sollinger, *Mikrochim. Acta (Wien)* **III**, 233–245, 247–258 (1990).
- [4] R.A. Fletton, R.K. Harris, A.M. Kenwright, R.W. Lancaster, K.J. Packer and N. Sheppard, *Spectrochim. Acta* **43A**, 1111–1120 (1987).
- [5] R.K. Harris, B.J. Say, R.R. Yeung, R.A. Fletton and R.W. Lancaster, *Spectrochim. Acta* **45A**, 465–469 (1989).
- [6] J.R. Powell, J.M. DeForrest, D.W. Cushman, B. Rubin and E.W. Petrillo, *Fed. Proc., Fed. Am. Soc. Exp. Biol.* **43**, 733 (1984).
- [7] J.S. Frye and G.E. Maciel, *J. Magn. Reson.* **48**, 125–131 (1982).
- [8] A. Pines, M.G. Gibby and J.S. Waugh, *J. Chem. Phys.* **56**, 1776–1777 (1972).
- [9] A. Pines, M.G. Gibby and J.S. Waugh, *Chem. Phys. Lett.* **15**, 373–376 (1972).
- [10] A. Pines, M.G. Gibby and J.S. Waugh, *J. Chem. Phys.* **59**, 569–590 (1973).
- [11] R.R. Ernst, *Rev. Sci. Instr.* **36**, 1689–1695 (1965).
- [12] R.R. Ernst and W.A. Anderson, *Rev. Sci. Instr.* **36**, 1696–1706 (1965).
- [13] A. Burger and R. Ramberger, *Mikrochim. Acta (Wien)* **II**, 259–271 (1979).
- [14] S.J. Opella and L.M. Gierasch, in *The Peptides: Analysis Synthesis, Biology*, Vol. 7 (V.J. Hruby, Ed.), pp. 418–422. Academic Press, San Diego (1985).
- [15] C.A. Fyfe, *Solid State NMR for Chemists*, p. 536. CFC Press, Guelph, Ontario (1983).

[Received for review 10 May 1993;  
revised manuscript received 1 July 1993]